4226–4239 *Nucleic Acids Research, 2019, Vol. 47, No. 8* *Published online 25 February 2019*
doi: 10.1093/nar/gkz111

Depletion of *S*-adenosylmethionine impacts on ribosome biogenesis through hypomodification of a single rRNA methylation

Kensuke Ishiguro, Taiga Arai and Tsutomu Suzuki*

Department of Chemistry and Biotechnology, Graduate School of Engineering, University of Tokyo, 7-3-1 Hongo, Bunkyo-ku, Tokyo 113-8656, Japan

Received January 28, 2019; Editorial Decision February 03, 2019; Accepted February 18, 2019

ABSTRACT

***S*-adenosylmethionine (SAM) is an essential metabolite and a methyl group donor in all living organisms. The intracellular SAM concentration is tightly regulated, and depletion causes hypomethylation of substrates, growth defects and pathological consequences. In the emerging field of epitranscriptomics, SAM-dependent RNA methylations play a critical role in gene expression. Herein, we analyzed the methylation status of ribosomal RNAs (rRNAs) and transfer RNAs (tRNAs) in *Escherichia coli* Δ*mtn* strain in which cellular SAM was down-regulated, and found hypomodification of several methylation sites, including 2′-*O*-methylation at position 2552 (Um2552) of 23S rRNA. We observed severe growth defect of the Δ*mtn* strain with significant accumulation of 45S ribosomal precursor harboring 23S rRNA with hypomodified Um2552. Strikingly, the growth defect was partially restored by overexpression of *rlmE* encoding the SAM-dependent methyltransferase responsible for Um2552. Although SAM is involved not only in rRNA methylation but also in various cellular processes, effects on ribosome biogenesis contribute substantially to the observed defects on cell proliferation.**

INTRODUCTION

S-adenosylmethionine (SAM) is a central metabolite involved in various cellular processes. SAM functions as a methyl donor for macromolecules and metabolites in reactions catalyzed by a wide variety of methyltransferases (1). SAM is also used in various cellular reactions utilizing a methylene group for fatty acid synthesis, a sulfur group for biotin synthesis, a ribosyl group for transfer RNA (tRNA) modification, an aminocarboxypropyl group for RNA modifications and an aminopropyl group for polyamine synthesis (1–7). SAM-dependent methylation is involved in epigenetic regulation through DNA and histone methylations, and affects diverse cellular processes from animal development and differentiation to brain functions (8–13). In addition, recent studies reveal that SAM-dependent methylation plays a critical role in RNA methylations in diverse biological contexts. The concept of the 'epitranscriptome' highlights the importance of RNA methylation as a regulatory element in gene expression (14–17).

The ribosome is an essential ribonucleoprotein complex that translates genetic information from messenger RNA (mRNAs) into proteins in all living organisms. In bacteria, the mature 70S ribosome consists of small subunit (30S) and large subunit (50S), each composed of ribosomal RNAs (rRNAs) and ribosomal proteins (r-proteins). These subunits can be non-enzymatically reconstituted *in vitro* from their individual components, albeit slowly under non-physiological conditions (18–20). However, in cells, ribosomes are synthesized rapidly and efficiently under physiological conditions because ribosome assembly is coupled with rRNA transcription, and the process is assisted enzymatically by various non-ribosomal 'assembly factors' including RNA helicases, GTPases, rRNA-modifying enzymes and protein chaperones (21–23). Since ribosome biogenesis is an energy-consuming process, it is tightly regulated by cellular growth and stress conditions (24). Under amino acid starvation conditions, fewer rRNAs and r-proteins are produced due to transcriptional regulation triggered by the alarmones, (p)ppGpp in bacteria (25,26). In addition to transcriptional regulation, it is proposed that ribosome biogenesis is also regulated in complex processes of ribosome assembly (27), but the precise mechanism remains to be elucidated.

In *Escherichia coli*, late stages of 50S subunit assembly require several assembly factors including RNA helicases (DeaD and DbpA), a GTPase (ObgE and Der) and a rRNA methyltransferase (RlmE) (21). RlmE is a SAM-dependent methyltransferase responsible for 2′-*O*-methylation of U2552 (Um2552) of Helix 92 in domain V of 23S rRNA (28). RlmE is a highly conserved methyltransferase in all domains of life, as well as in organelles, indicat-

*To whom correspondence should be addressed. Tel: +81 3 5841 8752; Fax: +81 3 5841 0550; Email: ts@chembio.t.u-tokyo.ac.jp

ing the functional importance of this enzyme. Deletion of *rlmE* results in a severe growth defect with cold sensitivity and accumulation of the 45S precursor (29). The precursor sediments at 45S at low Mg^{2+} concentrations, gradually increases in density with increasing Mg^{2+}, and almost comigrates with the 50S subunit at high Mg^{2+} concentration, because the 45S precursor has structurally flexible regions that undergo conformational changes upon Mg^{2+} binding (30). Structural probing of 23S rRNA in the 45S precursor revealed that domains III and IV are flexible at low Mg^{2+} concentration. Biochemical analyses revealed that the 45S precursor lacks several r-proteins including L16, L18, L25, L31, L33, L35 and L36 that reside in the upper region of the interface side of 50S, including the central protuberance (CP) (30). Curiously, we observed a strong genetic interaction between *rlmE* and *rpmJ* (encoding L36). Moreover, we partially reconstituted the 50S subunit *in vitro* from the 45S precursor triggered by RlmE-mediated Um2552 formation in the presence of the wash fraction of crude ribosomes (30). This was the first demonstration of the enzymatic formation of a ribosomal subunit *in vitro* from its precursor via the action of an assembly factor. Mechanistically, RlmE-mediated Um2552 formation promotes interdomain interactions between helices 71 and 92, because Um2552 favors C3′ *endo* ribose puckering and stabilizes the Um2552-C2556-U1955 base triple, followed by recruitment of L36 via correct positioning of helix 91. L36 stabilizes surrounding helices, thereby facilitating incorporation of late binders. This finding let us to speculate that late steps of 50S assembly may be regulated by RlmE-mediated Um2552 formation under some physiological conditions.

In the present study, we analyzed the methylation status of rRNAs and tRNAs in an *E. coli* strain in which the cellular SAM concentration is down-regulated, and identified hypomodification of several methylation sites, including Um2552 of 23S rRNA. We observed a severe growth defect of this strain, with significant accumulation of the 45S precursor with hypomodified Um2552. Notably, *rlmE* overexpression partially reversed this defect, and reduced accumulation of the 45S precursor. SAM depletion significantly impacts on ribosome biogenesis and effects on ribosome biogenesis contribute substantially to the observed defects on cell proliferation, though SAM is involved not only in rRNA methylation but also in various cellular processes.

MATERIALS AND METHODS

Strains and plasmid construction

Single-deletion strains with kanamycin resistance markers (Keio collection) (31) and their parental strain BW25113 were obtained from the Genetic Stock Research Center, National Institute of Genetics, Japan. *Escherichia coli* DY330 strains [W3110, Δ*lacU*169, *gal*490, *pgl*8 and λc1857(*cro-bioA*)] used for expression of RlmE-SPA were obtained from Thermo Scientific Open Biosystems. We disrupted *rlmE* in BW25113 using the chloramphenicol acetyltransferase (cat) cassette by one-step gene inactivation (32) to yield strain Δ*rlmE*::Cm^r. Single-colony isolation was repeated twice for all strains constructed in this study. Genotyping of knockout strains was conducted by colony polymerase chain reaction (PCR). To construct the double knockout strain Δ*mtn*/Δ*rlmE,* Δ*rlmE*::Cm^r was introduced into the Δ*mtn*::Km^r strain by P1 transduction. The double knockout strain Δ*rna*/Δ*rlmE* was prepared as previously described (30). To generate expression plasmids for RNA methyltransferases, each open reading frame was PCR-amplified from the *E. coli* genome using a set of primers listed in Supplementary Table S1. Amplified products were inserted into the XhoI/PstI sites of the pBAD/myc-HisA vector (Invitrogen). For expression of these constructs, 1 mM L-arabinose and 100 μg/ml ampicillin were added before inoculation of the preculture.

Analysis and preparation of ribosomes and ribosomal subunits by SDG

For profiling ribosomal fractions, *E. coli* strains were cultivated in 200 ml LB medium with vigorous shaking until the absorbance at 600 nm (A_{600}) reached 0.4–0.6. Cells were then quickly chilled on ice for 10 min, and 30ml culture was harvested by centrifugation. Extraction and analysis of ribosomal fractions was carried out as previously described (30). The cell pellet from a 30 ml culture was resuspended in 1 ml of Ribosomes (RBS) buffer A [0.5 mM $Mg(OAc)_2$, 200 mM NH_4Cl, 20 mM 4-(2-hydroxyethyl)-1-piperazineethanesulfonic acid (HEPES)-KOH (pH 7.6) and 6 mM β-mercaptoethanol] or RBS buffer B [10 mM $Mg(OAc)_2$, 100 mM NH_4Cl, 20 mM HEPES-KOH (pH 7.6) and 6 mM β-mercaptoethanol] and lysed by lysozyme treatment (1.5 mg/ml) followed by three rounds of freezing and thawing. The cell lysate was cleared by centrifugation at 20 000 × *g* for 15 min at 4°C. The supernatant was layered on top of a sucrose gradient (10–40%, w/v) in RBS buffer A or B and separated by ultracentrifugation in a Beckman SW-28 Rotor at 20 000 rpm for 14 h at 4°C, or in a Beckman SW-41 Rotor at 37 000 rpm for 5 h at 4°C. Separated ribosomal subunits were fractionated using a Piston Gradient Fractionator (BIOCOMP), and the A_{260} was measured using an AC-5200 UV monitor (ATTO).

For preparation of ribosomal subunits and precursors, *E. coli* strains were cultivated in 1 L LB medium and harvested by centrifugation as described above. The cell pellet was ground with alumina (weighing two to three times as much as the cell pellet) in a mortar and pestle for 10 min at 4°C. The ground cell pellet was resuspended in 20 ml of RBS buffer C [10 mM $Mg(OAc)_2$, 30 mM NH_4Cl, 20 mM HEPES-KOH (pH 7.6) and 6 mM β-mercaptoethanol] and centrifuged at 4400 × *g* for 30 min at 4°C. The supernatant was ultracentrifuged in a Beckman 70 Ti rotor at 19 500 rpm for 45 min at 4°C to remove cell debris. The supernatant was then ultracentrifuged in a 70 Ti rotor at 35 000 rpm for 4 h at 4°C to obtain crude ribosomes. These were resuspended in RBS buffer A, layered on top of a sucrose gradient (10–50%, w/v) in RBS buffer A and ultracentrifuged in a Beckman SW-28 Rotor at 25 000 rpm for 15 h at 4°C. The sucrose gradient was fractionated using a Piston Gradient Fractionator, and the A_{260} of each fraction was measured using a SpectraMax Microplate Reader (Molecular Devices). The fractions corresponding to 30S and 50S subunits or 45S precursor were pooled and recovered by ultracentrifugation in a Beckman 70 Ti rotor at 40 000 rpm for

24 h at 4°C in RBS buffer B. The pellet was resuspended in RBS buffer D [0.5 mM $Mg(OAc)_2$, 100 mM NH_4Cl, 20 mM HEPES-KOH (pH 7.6) and 6 mM β-mercaptoethanol] and stored at –80°C.

Tricine SDS PAGE

Ribosomal proteins were extracted from each ribosomal molecule with acetic acid and precipitated in acetone as previously described (33). Proteins were subjected to Tris-tricine/urea 18% polyacrylamide gel electrophoresis (PAGE) at 90 V for 13 h (34). The gel was stained with SYPRO Ruby (Molecular Probes) and visualized on an FLA-7000 imaging analyzer (FujiFilm).

Mass spectrometry of rRNA modifications

rRNAs were extracted from ribosomal molecules with TRIzol LS reagent (ThermoFisher Scientific). For site-specific analysis of rRNA methylations, synthetic DNAs complementary to rRNA segments surrounding the target modification were designed (Supplementary Table S1). The rRNAs (20 pmol) extracted from each molecule were mixed with synthetic DNA (200 pmol) in 50 mM HEPES-KOH (pH 7.6) and 100 mM KCl. The mixture was heated at 90°C for 5 min, then gradually cooled to 37°C (−1°C/min) to allow DNA to form a heteroduplex with rRNA. Uncovered regions of rRNA were then digested with 50 units of RNase T_1 (ThermoFisher Scientific) and 50 ng of RNase A for 60 min on ice. The heteroduplex was extracted with phenol/chloroform (pH 7.9), precipitated with ethanol and resolved by 15% denaturing PAGE, followed by staining with SYBR Gold (Molecular Probes). The heteroduplex was excised from the gel, eluted from the gel piece for 5 h at 37°C in elution buffer [1 mM ethylenediaminetetraacetic acid, 0.1% sodium dodecyl sulphate (SDS) and 0.4 M NaOAc (pH 5.2)], and precipitated with ethanol. The heteroduplex (500 fmol) was digested with 10 units of RNase T_1 in 20 mM NH_4OAc (pH 5.3) or 10 ng of RNase A in 20 mM NH_4OAc (pH 7.0) at 37°C for 60 min. Digested RNA was mixed with an equal amount of 0.1 M triethylamine acetate and subjected to capillary LC/nano ESI-MS on an LTQ Orbitrap mass spectrometer (Thermo Scientific) equipped with a splitless nanoflow high-performance LC (HPLC) system (DiNa, KYA Technologies) as previously described (35).

Mass spectrometry of tRNA modifications

Escherichia coli cells from a 5 ml culture were suspended in 300 μl RBS buffer A containing 1 mg/ml lysozyme and incubated on ice for 15 min. The cell lysate was mixed with 900 μl of TRIzol LS reagent (ThermoFisher Scientific), lysed by three rounds of freezing and thawing, mixed with 240 μl chloroform and precipitated with isopropanol. Total RNA (5 μg) was resolved by 15% denaturing PAGE and visualized by staining with SYBR Gold (Molecular Probes). The tRNA fraction was excised from the gel, eluted from the gel piece for 5 h at 37°C in elution buffer and precipitated with ethanol. To digest tRNAs into nucleosides, the tRNA fraction (1.0 μg) was incubated at 37°C for 60 min in a 20 μl solution with 0.1 unit nuclease P1 (Wako Pure Chemical Industries), followed by addition of 1 μl of 1 M ammonium bicarbonate (pH 8.2) and 0.2 unit Phosphodiesterase I (Worthington) and incubated at 37°C for 60 min, then 0.1 unit of bacterial alkaline phosphatase (BAP from *E. coli* C75, Wako Pure Chemical Industries) was added, and incubated at 37°C for 60 min. Nucleosides were dried *in vacuo*, dissolved in 90% acetonitrile (10% water), and subjected to hydrophilic interaction liquid chromatography (HILIC) coupled ESI-MS using a Q Exactive hybrid Quadrupole-Orbitrap mass spectrometer (Thermo Fisher Scientific) equipped with an ESI source and an Ultimate 3000 liquid chromatography system (Dionex) (36). To separately detect m^1G and Gm, nucleosides were analyzed by RPC/ESI-MS condition using a polymer-coated core shell column containing resin with adamantyl group (CAPCELL CORE ADME column, 2.7 μm particle size, 2.1 × 150 mm, Osaka soda). LC/MS condition was the same as described (35). The relative abundance of each nucleoside was normalized against the respective unmodified nucleoside. In the case of ms^2i^6A, frequency was measured from the proportion of the ms^2i^6A peak area to the total peak areas of ms^2i^6A and i^6A, because the ionization efficiencies of these nucleosides were almost identical in our measurement(37).

To analyze modification status in individual tRNAs, we isolated tRNAs for Phe, His, Arg2, Arg3, Lys, Met and Val2B from both WT and Δ*mtn* strains by reciprocal circulating chromatography (38). The isolated tRNAs were digested by RNase T1 and analyzed by RNA-MS as described above.

Reverse transcription-quantitative PCR

Total RNA (25 ng) was treated with RNase-free DNase (RQ1 DNase, Promega) then converted to complementary DNAs (cDNAs) via reverse transcription with a Transcriptor First Strand cDNA Synthesis Kit (Roche). cDNAs were mixed with KAPA SYBR (KAPA Biosystems) and 2 pmol primers (Supplementary Table S1). Quantitative PCR analysis was carried out with a sets of primers (Supplementary Table S1) using a Light Cycler 480 instrument (Roche) and KAPA SYBR (KAPA Biosystems). *idnT* was used as a reference gene as described (39).

In vitro methylation assay

Recombinant RlmE was prepared as previously described (30). The 45S precursor and 50S subunit were prepared from the Δ*rna*/Δ*rlmE* strain as described above. Ten pmol of the 45S precursor or 50S subunit was incubated for 2 h at 37°C with 2 pmol RlmE in the presence of various concentration of SAM in 20 μl reaction mixture containing 50 mM Hepes-KOH (pH7.6), 50 mM KCl, 5 mM $MgCl_2$ and 1 mM dithiothreitol (DTT). The SAM concentration ranged from 3 to 3000 μM. After the reaction, the rRNAs were extracted from the mixture with TRIzol LS reagent (ThermoFisher Scientific), followed by the site-specific analysis of rRNA methylations as described above. We also carried out a time-course analysis in the presence of 3000 μM SAM, and confirmed the reaction was not saturated even after 2 h.

RESULTS

SAM depletion impacts on ribosomal 50S subunit assembly

In our previous study, we showed that late steps of 50S assembly are triggered by a single 2′-*O*-methylation at U2552 of 23S rRNA mediated by RlmE. Given that RlmE is a SAM-dependent methyltransferase, we hypothesized that 50S assembly may be regulated by the cellular SAM concentration. To evaluate the effect of SAM depletion on ribosome biogenesis, we manipulated the SAM metabolic cycle. As shown in Supplementary Figure S1, SAM is supplied by both *de novo* synthesis and a recycle pathway. SAM is synthesized *de novo* from adenosine triphosphate (ATP) and methionine (Met), catalyzed by MetK. Met is obtained from the medium as a nutrient, and also synthesized *de novo* through homocysteine (Hcy). SAM is then used by various methyltransferases as a methyl donor for production of *S*-adenosylhomocysteine (SAH). In the SAM recycle pathway, SAH is then metabolized to Met via three consecutive reactions. Initially, SAH is converted to *S*-ribosylhomocysteine (SRH) by SAH nucleosidase (Mtn). Deletion of the *mtn* gene in *E. coli* decreased the cellular SAM concentration to one-third that in WT cells (40). Thus, we used Δ*mtn* as a model strain with a low SAM concentration.

The Δ*mtn* strain grew slower than the WT strain, and exhibited a cold sensitive phenotype (Figure 1A), indicating that SAM depletion affects various cellular processes. To confirm that this phenotype is caused by *mtn* deletion, we rescued the Δ*mtn* strain using plasmid-encoded *mtn*, and the slow growth phenotype was indeed recovered (Figure 1B). The result ruled out the possibility that the phenotype was caused by polar effects of flanking genes affected by *mtn* deletion.

Next, we analyzed ribosomal subunits in the Δ*mtn* strain cultured at 22°C using sucrose density gradient (SDG) centrifugation. Strikingly, in this strain, we found a curious molecule that sedimented at 45S at low Mg^{2+} concentration, but increased in density and co-migrated with the 50S subunit at high Mg^{2+} concentration (Figure 1C). Given that mature 50S is able to associate with 30S to form the tightly coupled 70S ribosome at 10 mM Mg^{2+}, the molecule sedimenting at 50S in this Mg^{2+} concentration cannot associate with the 30S subunit (Figure 1C). We also confirmed the absence of L36 in the molecule (Figure 1D), which is a characteristic feature of the 45S precursor. Based on these findings, we concluded that the molecule accumulated in the Δ*mtn* strain is the 45S precursor. When the Δ*mtn* strain was rescued by plasmid-encoded *mtn*, the 45S precursor less-accumulated and the 50S subunit increased (Supplementary Figure S2).

We then examined accumulation of the 45S precursor in the Δ*mtn* strain in response to culture temperature (Figure 1E and Supplementary Figure S3). The 45S precursor accumulated at low temperature, and gradually decreased at higher temperature, with concomitant accumulation of the 50S subunit. Judging from the optical density ratio of ribosomal subunits, an equimolar ratio of 50S and 30S subunits was maintained in the Δ*mtn* strain cultured at different temperatures, indicating that the 45S precursor is efficiently converted to 50S subunit at higher culture temperature.

We next examined whether SAM depletion directly influences the growth phenotype of the Δ*mtn* strain. In the Δ*mtn* strain, SAM is not recycled, but supplied by *de novo* synthesis from Met and ATP catalyzed by MetK. We cultured WT and Δ*mtn* strains in M9 medium supplemented with amino acids, and compared their growth with or without Met (Figure 1F). The Δ*mtn* strain grew much slower than the WT strain in the absence of Met, presumably because *de novo* synthesis of SAM was impaired due to Met starvation. When Met was added to the medium, growth of the Δ*mtn* strain was restored, indicating that Met addition increased the cellular SAM concentration. Under these culture conditions, ribosomes were profiled by SDG analysis (Figure 1G). The 45S precursor accumulated in the absence of Met was reduced in the presence of Met. Therefore, 45S precursor accumulation resulted from SAM depletion in the Δ*mtn* strain.

Hypomodification of rRNA modifications in SAM-depleted cells

Escherichia coli 16S and 23S rRNAs contain 36 residues modified post-transcriptionally, of which 24 are methylated (Supplementary Figure S4) (21). To identify the methylation sites in rRNAs that are down-regulated upon SAM depletion, we employed capillary liquid chromatography (LC)-nano-electrospray ionization (ESI)-mass spectrometry (RNA-MS) to analyze all methylation sites in both 16S and 23S rRNAs isolated from the Δ*mtn* strain. The 30S, 45S and 50S ribosomal subunits from both WT and Δ*mtn* strains were separately isolated from the SDG fractions, and rRNAs from each molecule were extracted. RNA fragments containing each methylation site were detected by RNA-MS, and a modification frequency for each site was precisely measured from the mass chromatographic peak intensity ratio of methylated versus unmethylated fragments. We successfully determined the modification frequency of all known methylation sites; 10 sites in 16S rRNA (Table 1 and Supplementary Figure S5) and 14 sites in 23S rRNA (Table 2 and Supplementary Figure S6). In the 16S rRNA of WT 30S subunit, the methylation frequencies of the 10 sites ranged from 40 to 100%. Upon SAM depletion in the Δ*mtn* strain, two sites, 5-methylcytidine (m^5C) at position 1407 and 3-methyluridine (m^3U) at position 1498, were significantly decreased in frequency from 89 ± 2.6% and 72 ± 13% to 41 ± 4.7% and 42 ± 4.6%, respectively (Table 1 and Figure 2A). In the 23S rRNA of the WT 50S subunit, the methylation frequencies of all 14 sites were >90%. In the Δ*mtn* 45S species, four sites, 5-methyluririne (m^5U) at position 747, 3-methylpseudouridine ($m^3\Psi$) at position 1915, m^5U at position 1939 and Um at position 2552, were markedly decreased in frequency (Table 2 and Figure 2B). For m^5U747, its frequency in Δ*mtn* 45S (60%) remained unchanged in Δ*mtn* 50S (61%), whereas the frequency of $m^3\Psi1915$ in Δ*mtn* 45S (30%) was increased in Δ*mtn* 50S (86%). Because RlmH recognizes the 70S ribosome and introduces $m^3\Psi1915$ (41), this modification is not introduced in the 45S precursor that cannot associate with the 30S subunit. The frequency of m^5U1939 was slightly lower in Δ*mtn*

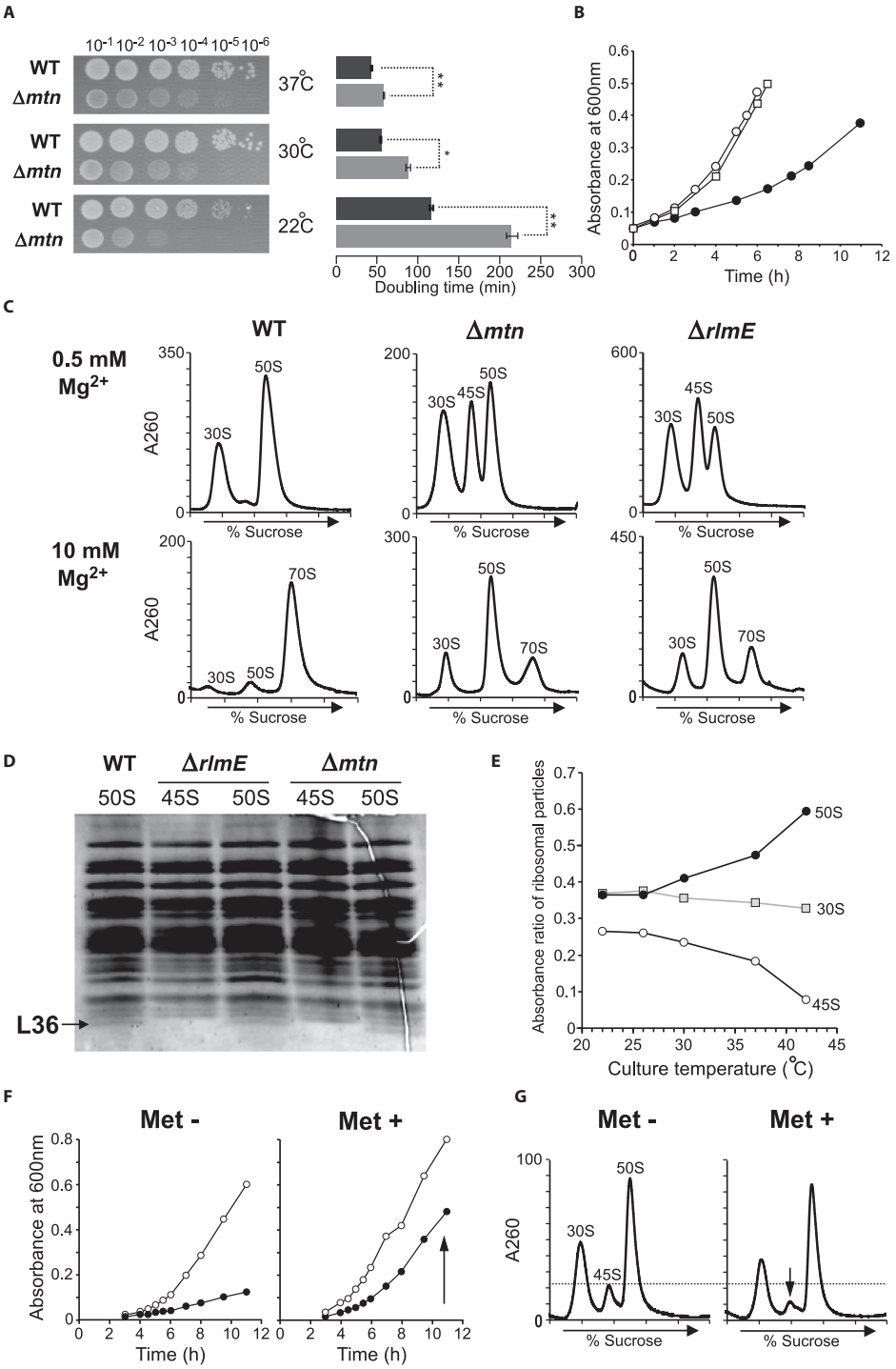

Figure 1. The ribosomal 45S precursor accumulates in Δ*mtn* strain. (**A**) Growth properties of WT and Δ*mtn* strains. (Left) Overnight full-growth cultures were serially diluted (OD_{600} from 10^{-1} to 10^{-6}), spotted onto LB plates and cultivated at 37, 30 or 22°C. (Right) The doubling time at each temperature was measured. Data represent average values ± SD from biological triplicates. Asterisks indicate the *P*-value from two-tailed *t*-tests (*$P < 0.01$, **$P < 0.001$). (**B**) Growth curves of WT (open squares), Δ*mtn* (closed circles), and the Δ*mtn* strain complemented with plasmid-encoded *mtn* (open circles) cultured at 22°C in LB medium. (**C**) Sucrose density gradient (SDG) profiles of ribosomes from WT, Δ*mtn* and Δ*rlmE* strains performed at low Mg^{2+} concentration (0.5 mM) and high Mg^{2+} concentration (10 mM). All strains were cultured at 22°C in LB medium. The *y*-axis represents milli-absorbance units at 260 nm. (**D**) Ribosomal proteins of the 45S precursor and the 50S subunit from WT, Δ*rlmE* and Δ*mtn* strains resolved by Tricine-SDS-PAGE. The gel was stained with SYPRO Ruby. L36 is indicated by an arrow. All strains were cultured at 22°C in LB medium. (**E**) Absorbance ratio of 30S (gray squares), 45S (open circles) and 50S (closed circles) species relative to total ribosomes at various temperatures. Ratios were calculated from the peak area in the SDG profiles described in Supplementary Figure S3. (**F**) Growth curves of WT (open circle) and Δ*mtn* (close circle) strains cultured at 30°C in M9 medium supplemented with 18 amino acids (without Met and Cys) (Left panel) or 19 amino acids (without Cys) (Right panel). (**G**) SDG profiles of ribosomes from the Δ*mtn* strain cultured at 30°C in M9 medium supplemented with 18 amino acids (without Met and Cys) (Left panel) or 19 amino acids (without Cys) (Right panel).

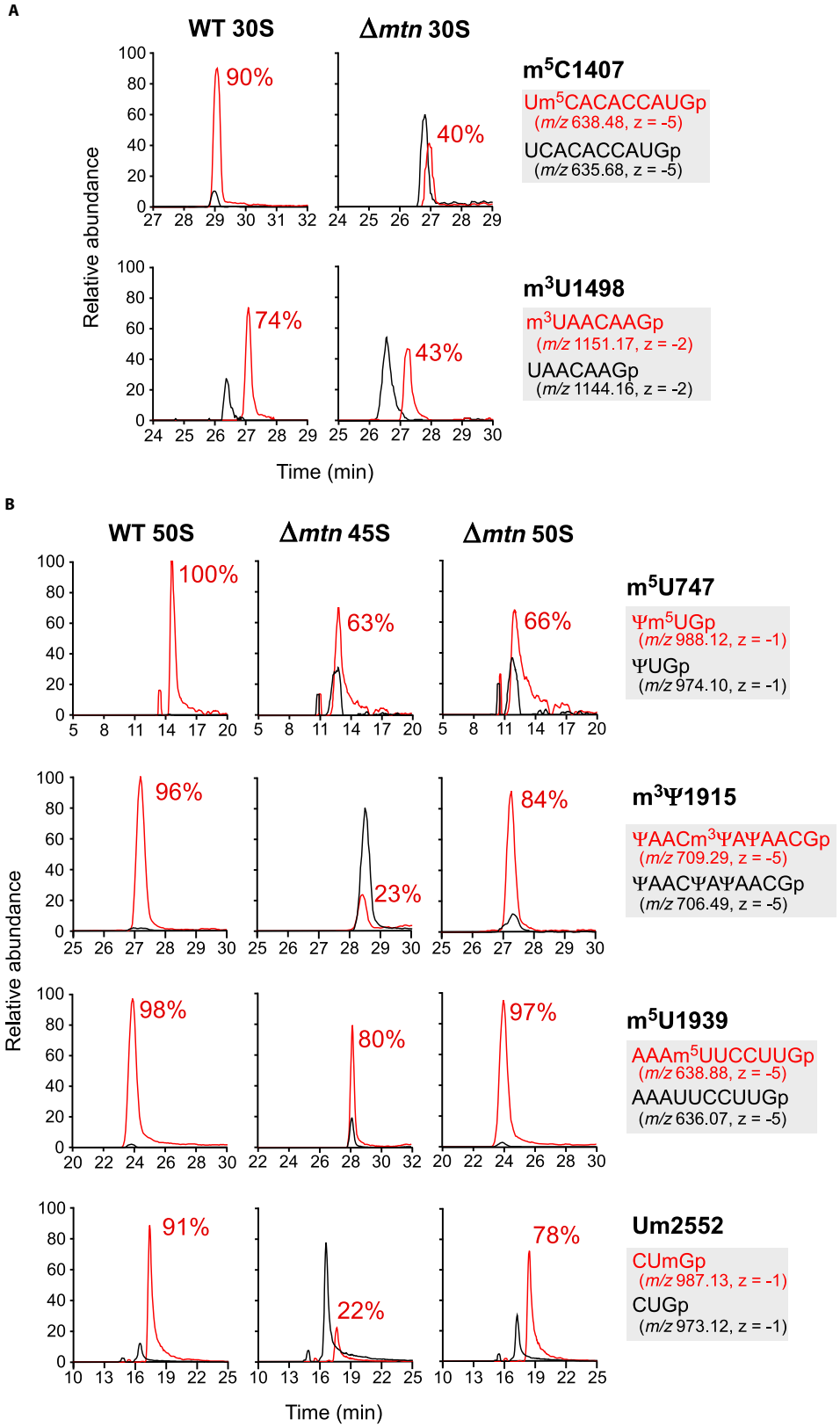

Figure 2. Status of rRNA methylations upon SAM depletion. (**A**) MS analyses of m^5U1407 (upper panels) and m^3U1498 (lower panels) in 16S rRNA from WT 30S (left panels) and Δ*mtn* 30S (right panels). Extracted ion chromatograms (XICs) of the indicated negative ions of the RNase T_1-digested fragments with (red lines) or without (black lines) target methylation are shown. (**B**) MS analyses of four methylations in 23S rRNA from WT 50S (left panels), Δ*mtn* 45S (center panels) and Δ*mtn* 50S (right panels). XICs of the indicated negative ions of the RNase T_1-digested fragments with (red lines) or without (black lines) target methylation are shown.

45S than in Δ*mtn* 50S, because RlmD introduces m^5U1939 during late stages of 50S assembly (42). Regarding Um2552, we observed a significant reduction in frequency to 28 ± 16% in Δ*mtn* 45S, and a recovery to 81 ± 8.7% in Δ*mtn* 50S. Because hypomethylation of Um2552 is a structural characteristic of the 45S precursor, accumulation of the 45S precursor in the Δ*mtn* strain can be explained by the low Um2552 frequency of 23S rRNA.

If expression level of *rlmE* is affected by SAM depletion, the 45S precursor should accumulate. We therefore measured the steady-state level of *rlmE* mRNA in the Δ*mtn* strain by reverse transcription-quantitative PCR. The relative ratio of *rlmE* mRNA in Δ*mtn* versus WT was 1.1 ± 0.1, suggesting that *rlmE* mRNA was not affected by SAM depletion in the Δ*mtn* strain. Therefore, RlmE is a methyltransferase sensitive to cellular SAM concentration, and regulates 50S assembly.

Alteration of tRNA modifications in SAM-depleted cells

Escherichia coli tRNAs contain 32 different types of modified nucleosides, including 16 species of methylmodifications (43–45). We investigated whether tRNA modifications are also affected by SAM depletion in the Δ*mtn* strain by subjecting tRNA fractions obtained from WT and Δ*mtn* strains to total nucleoside analysis using LC/MS. We detected 28 tRNA modifications species and two precursors, and compared the relative abundance of each modification in the two strains (Figure 3A; Supplementary Figures S7 and S8). Several methyl modifications, including 7-methylguanosine (m^7G), 2′-*O*-methylguanosine (Gm), m^5U, 5-methylaminomethyluridine (mnm^5U) and 2-methylthio-N^6-isopentenyladenosine (ms^2i^6A), were down-regulated upon SAM depletion in the Δ*mtn* strain, whereas other methyl modifications remained unchanged, suggesting that tRNA methylations are differentially regulated by cellular SAM concentration. In response to a reduction of ms^2i^6A, N^6-isopentenyladenosine (i^6A), a precursor of ms^2i^6A, accumulated in the Δ*mtn* strain (Figure 3B), indicating that 2-methylthiolation of ms^2i^6A, catalyzed by MiaB (46), is affected under low SAM concentrations in the cell. We also observed low levels of queuosine (Q) and its precursor epoxyqueuosine (oQ) in the Δ*mtn* strain. By contrast, 7-aminomethyl-7-deazaguanosine ($preQ_1$), a precursor of oQ, accumulated in the Δ*mtn* strain (Figure 3C). In the biogenesis of Q, SAM is used as a ribosyl donor, and QueA transfers the ribosyl group of SAM to preQ1 to synthesize oQ (47). Thus, accumulation of $preQ_1$ in this strain indicates that the QueA-mediated ribose transfer reaction is sensitive to cellular SAM concentration.

Here, we show distribution of tRNA modifications that were decreased in the Δ*mtn* strain (Supplementary Table S2). Among 6 tRNA modifications down-regulated in the Δ*mtn* strain, only m^5U54 is present in all tRNA species, whereas other modifications are present in specific tRNA species. To confirm the hypomodification of individual tRNA species, we isolated seven tRNA species from the Δ*mtn* strain, and analyzed the modification status by RNA-MS, and actually confirmed hypomodification of m^5U54, ms^2i^6A37 and Q34 in these tRNAs (Supplementary Figure S9A and B). Intriguingly, m^5U54 is differently regulated in these tRNAs. In the six tRNA species, m^5U54 was slightly reduced to 73–84%, whereas it was severely down-regulated to 5% in $tRNA^{His}$ (Supplementary Figure S9A), indicating that m^5U54 is $tRNA^{His}$ is highly sensitive to cellular SAM concentration. This additional experiment prompts us to further investigate tRNA modification status under low SAM level in the cell.

Overexpression of *rlmE* alleviates the defective growth phenotype of SAM-depleted cells

We observed that several methyl modifications in rRNAs and tRNAs were down-regulated in the Δ*mtn* strain. Given that accumulation of the 45S precursor is a prominent feature of this strain, we examined whether RlmE-mediated Um2552 formation promotes 50S assembly and restores the slow growth phenotype of the Δ*mtn* strain. To this end, we attempted to rescue the slow growth of the Δ*mtn* strain by overexpressing a series of RNA-modifying enzymes for which target modifications were down-regulated in the Δ*mtn* strain. When *rlmE* was overexpressed, the doubling time of the Δ*mtn* strain was reduced significantly (Figure 4A and B), whereas overexpression of other genes including *rlmC* (m^5U747), *rsmE* (m^3U1498), *rsmF* (m^5C1407), *miaB* (ms^2i^6A in tRNA) and *queA* (oQ in tRNA) did not restore the growth phenotype of this strain (Figure 4A). We next profiled ribosome in these constructs, and found that *rlmE* overexpression completely diminished 45S accumulation and increased 50S subunit, whereas other genes examined did not affect the ribosome profiles of the Δ*mtn* strain (Figure 4C). We next analyzed Um2552 frequencies in 23S rRNAs of the 45S precursor and 50S subunit isolated from the Δ*mtn* strain overexpressing *rlmE*. Upon overexpression of *rlmE*, Um2552 sites of the 45S and 50S were significantly increased in frequency from 28 ± 16% and 81 ± 8.7% (Table 2) to 51 and 95%, respectively (Figure 4D), indicating that *rlmE* overexpression efficiently introduces Um2552 and promotes 50S assembly. To confirm overexpression of *rsmF* and *rlmC*, we analyzed m^5C1407 and m^5U747 in the Δ*mtn* strain overexpressing *rsmF* and *rlmC,* respectively (Supplementary Figure S10). m^5C1407 was restored from 41 to 86% by *rsmF* overexpression, whereas m^5U747 was fully restored in both 45S and 50S subunit by overexpressing *rlmC*.

DISCUSSION

SAM is used as a methyl group donor for a wide variety of methyltransferases, and is involved in many essential biological processes (1). In DNA methylation, Dam methylase introduces N^6-methyldeoxyadenosine (m^6dA) in GATC motif, and this methylation plays a critical role in DNA replication initiation, methyl-directed mismatch repair and transcriptional regulation (48,49). In eukaryote, 5-methyldeoxycytidine (m^5dC) is a major epigenetic mark responsible for various processes including differentiation and reprogramming (13). SAM is also a methyl group donor for methylation of proteins and RNAs. In translational machineries, translational factors, tRNAs, rRNAs and r-proteins are methylated at numerous sites (43,50,51).

In the present study, to reduce the SAM concentration in the cell, we employed the *E. coli* Δ*mtn* strain which has

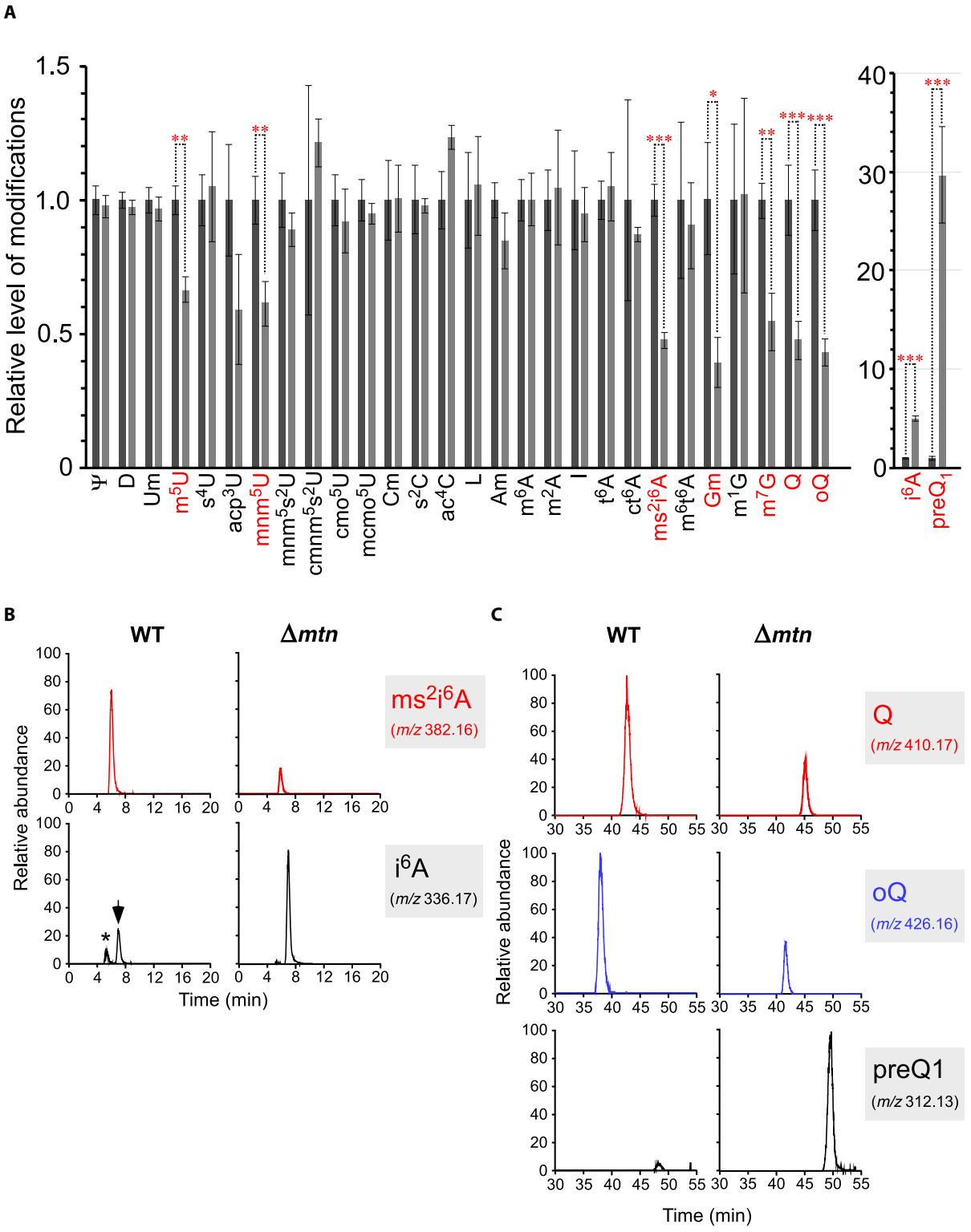

Figure 3. Status of tRNA methylations upon SAM depletion. (**A**) The relative abundance of tRNA modifications in the Δ*mtn* strain (light gray) versus the WT strain (dark gray) were measured by MS analysis of nucleosides. All modifications except for m^1G and Gm were analyzed by HILIC/ESI-MS, while m^1G and Gm were analyzed by RPC/ESI-MS using a polymer-coated core shell column containing resin with adamantyl groups (see 'Materials and Methods' section). The relative abundance of each nucleoside was normalized against the respective unmodified nucleoside. Data represent average values ± SD from biological triplicates. Asterisks indicate modifications for which the frequency was statistically decreased in the Δ*mtn* strain (*$P < 0.025$, **$P < 0.01$, ***$P < 0.001$). (**B**) XICs of the proton adducts of nucleosides for ms^2i^6A and i^6A in WT and Δ*mtn* strains. Asterisks represent unrelated fragments with the same *m/z* values. Frequency of ms^2i^6A was measured from the proportion of the ms^2i^6A peak area to the total peak areas of ms^2i^6A and i^6A, because the ionization efficiencies of these nucleosides were almost identical in our measurement (37). (**C**) XICs of the proton adducts of nucleosides for queuosine and its precursors in WT and Δ*mtn* strains. The relative abundance was normalized by the abundance of guanosine.

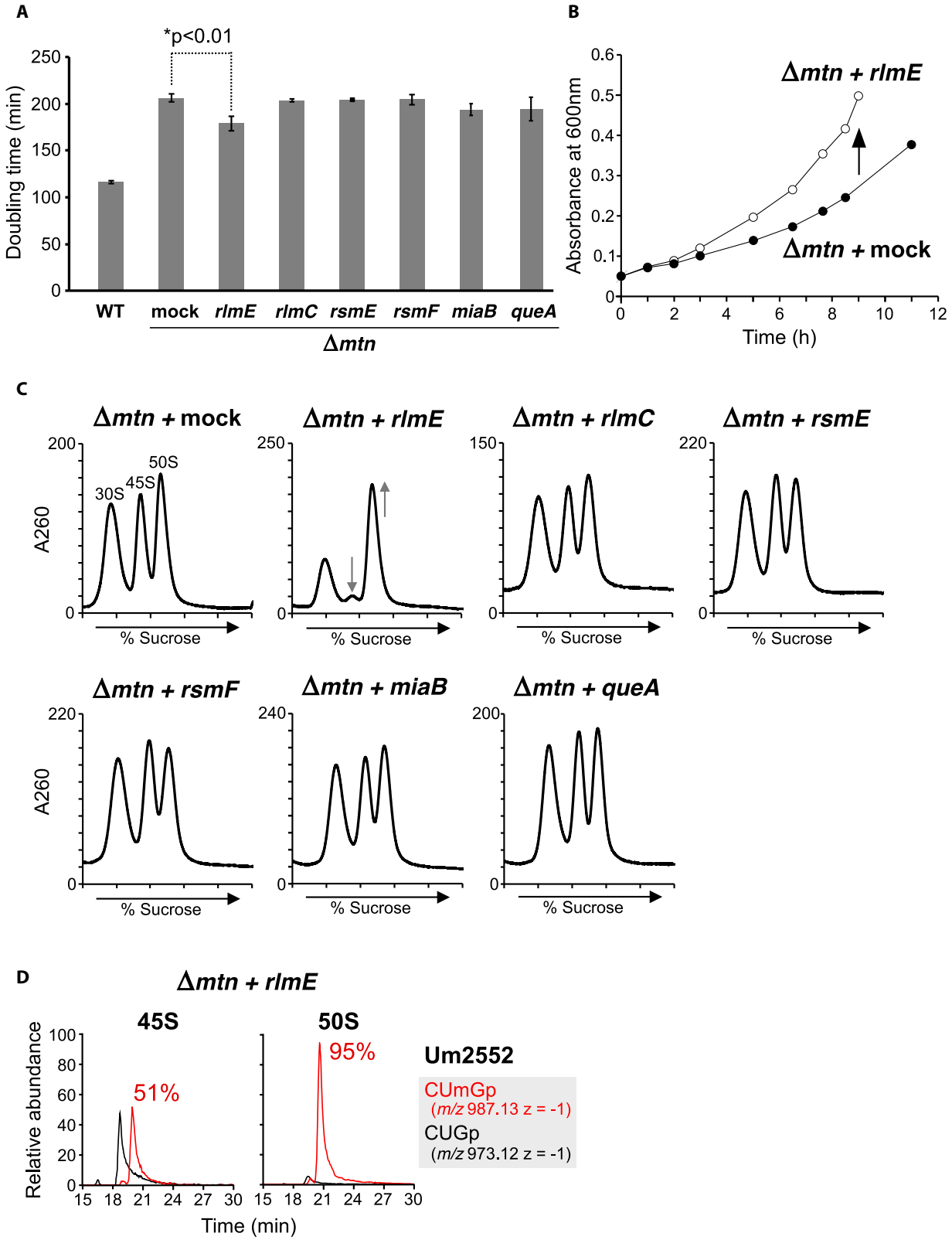

Figure 4. Overexpression of *rlmE* restores the growth phenotype of the Δ*mtn* strain. (**A**) Doubling time of WT and Δ*mtn* strains overexpressing different RNA-modifying enzymes. All strains were cultured at 22°C. Data represent average values ± SD from biological triplicates. Asterisks indicate *P*-values from two-tailed *t*-tests. (**B**) Growth curves of the Δ*mtn* strain overexpressing a mock gene (closed circles) and *rlmE* (open circles) cultured at 22°C in LB medium. (**C**) SDG profiles of ribosomes from Δ*mtn* strains overexpressing different RNA-modifying enzymes as indicated. All strains were cultured at 22°C. (**D**) Mass spectrometric analyses of Um2552 in 23S rRNAs in the 45S precursor (left panel) and 50S subunit (right panel) from the Δ*mtn* strain overexpressing *rlmE*. XICs of the indicated negative ions of the RNase T_1-digested fragments with (red lines) or without (black lines) Um2552.

Table 1. Modification frequencies of all methylated residues in 16S rRNA from wild-type and Δ*mtn* strains

Modification	Enzyme	WT 30S	Δ*mtn* 30S
m^7G527	RsmG	100	100
m^2G966	RsmD	100	100
m^5C967	RsmB	49 ± 9.9	50 ± 9.7
m^2G1207	RsmC	87 ± 2.8	82 ± 7.3
m^4Cm1402	RsmH, RsmI	40 ± 4.3	31 ± 4.0
m^5C1407	RsmF	89 ± 2.6	**41 ± 4.7**
m^3U1498	RsmE	72 ± 13	**42 ± 4.6**
m^2G1516	RsmJ	95 ± 3.4	97 ± 5.2
$m^{6,6}$A1518 1519	RsmA (KsgA)	90 ± 2.8	86 ± 9.3

The frequency of each modification as indicated on the right was calculated from the extracted ion chromatogram (XIC) peak intensity ratio between methylated and unmethylated RNA fragments. Data represent average values ± standard deviation (SD) from biological triplicates. Bold text represents modification frequencies that are decreased by a statistically significant amount in the Δ*mtn* strain ($P < 0.05$).

Table 2. Modification frequencies of all methylated residues in 23S rRNA from wild-type and Δ*mtn* strains

Modification	Enzyme	WT 50S	Δ*mtn* 45S	Δ*mtn* 50S
m^1G745	RlmA	100	100	100
m^5U747	RlmC	100	**60 ± 16**	**61 ± 13**
m^6A1618	RlmF	100	100	100
m^2G1835	RlmG	100	100	100
$m^3\Psi$1915	RlmH	96 ± 1.4	**30 ± 14**	**86 ± 2.9**
m^5U1939	RlmD	98 ± 0.3	**81 ± 3.5**	98 ± 0.8
m^5C1962	RlmI	100	100	100
m^6A2030	RlmJ	97 ± 0.9	94 ± 1.4	94 ± 0.2
m^7G2069	RlmKL	100	96 ± 1.7	96 ± 2.3
Gm2251	RlmB	99 ± 0.4	96 ± 2.2	93 ± 0.5
m^2G2445	RlmKL	100	100	100
Cm2498	RlmM	97 ± 0.2	96.1±0.4	98 ± 0.2
m^2A2503	RlmN	100	100	100
Um2552	RlmE	91 ± 5.2	**28 ± 16**	81 ± 8.7

The frequency of each modification as indicated on the right was calculated from the XIC peak intensity ratio between methylated and unmethylated RNA fragments. Data represent average values ± SD from biological triplicates. Bold text represents modification frequencies that are decreased by a statistically significant amount in Δ*mtn* strains ($P < 0.05$).

an intracellular SAM concentration of ∼100 μM, approximately one-third of that in WT cells (∼250 μM) (40). The Δ*mtn* strain exhibited slow growth and cold sensitive phenotypes because SAM is involved in many cellular processes, and SAM depletion impacts on various cellular processes. As expected, we observed that several methyl modifications in rRNAs and tRNAs were down-regulated in the Δ*mtn* strain. Most intriguingly, the growth phenotype and 45S accumulation of the Δ*mtn* strain was substantially restored by *rlmE* overexpression, but not by overexpression of any other methyltransferase genes examined in this study. This result clearly demonstrated that SAM depletion impacts on ribosome biogenesis via hypomethylation of Um2552, and regulates cell proliferation, even though SAM is involved not only in rRNA methylation but also in various cellular processes. Alternatively, there is another possibility that other assembly factors may sense cellular SAM concentration, and regulate RlmE-mediated Um2552 formation.

In addition to hypomethylation of Um2552, we found two sites in 16S rRNA and two sites in 23S rRNA that were hypomethylated in the Δ*mtn* strain. Since m^5C1407 and m^3U1498 are located in helix 44 of 16S rRNA, they likely contribute to P site function and/or intersubunit association with the 50S subunit. RsmF and RsmE introduce m^5C1407 and m^3U1498, respectively. Hypomethylation of m^3U1498 was also found in the 30S subunit isolated from the Δ*rlmE* strain (Supplementary Figure S11), indicating that RsmE-mediated m^3U1498 formation was affected by impaired 50S assembly in Δ*rlmE* strain, not by SAM depletion. By contrast, RsmF-mediated m^5C1407 formation was sensitive to SAM concentration, and passively regulated under SAM depletion. Lack of m^5C1407 in the Δ*rsmF* strain results in growth retardation (52), and lack of m^3U1498 in Δ*rsmE* strain causes a mild phenotype but loss in competition with the WT strain in co-culturing experiment (53). Thus, hypomethylation of these sites in the Δ*mtn* strain might directly affect ribosome quality and function, and thereby regulate translation under certain stress conditions. In 23S rRNA, in addition to Um2552, m^5U747 was also hypomethylated in the Δ*mtn* strain, implying that RlmC is sensitive to SAM concentration. Although m^5U747 is positioned in peptide exit tunnel and may have a role in translation fidelity, no obvious phenotype was evident for the Δ*rlmC* strain (54), suggesting m^5U747 hypomethylation has a limited influence on ribosome function. The low frequency of $m^3\Psi$1915 in the 45S precursor was restored in the 50S subunit, because $m^3\Psi$1915 is a 70S-specific modification introduced by RlmH. This observation can be ex-

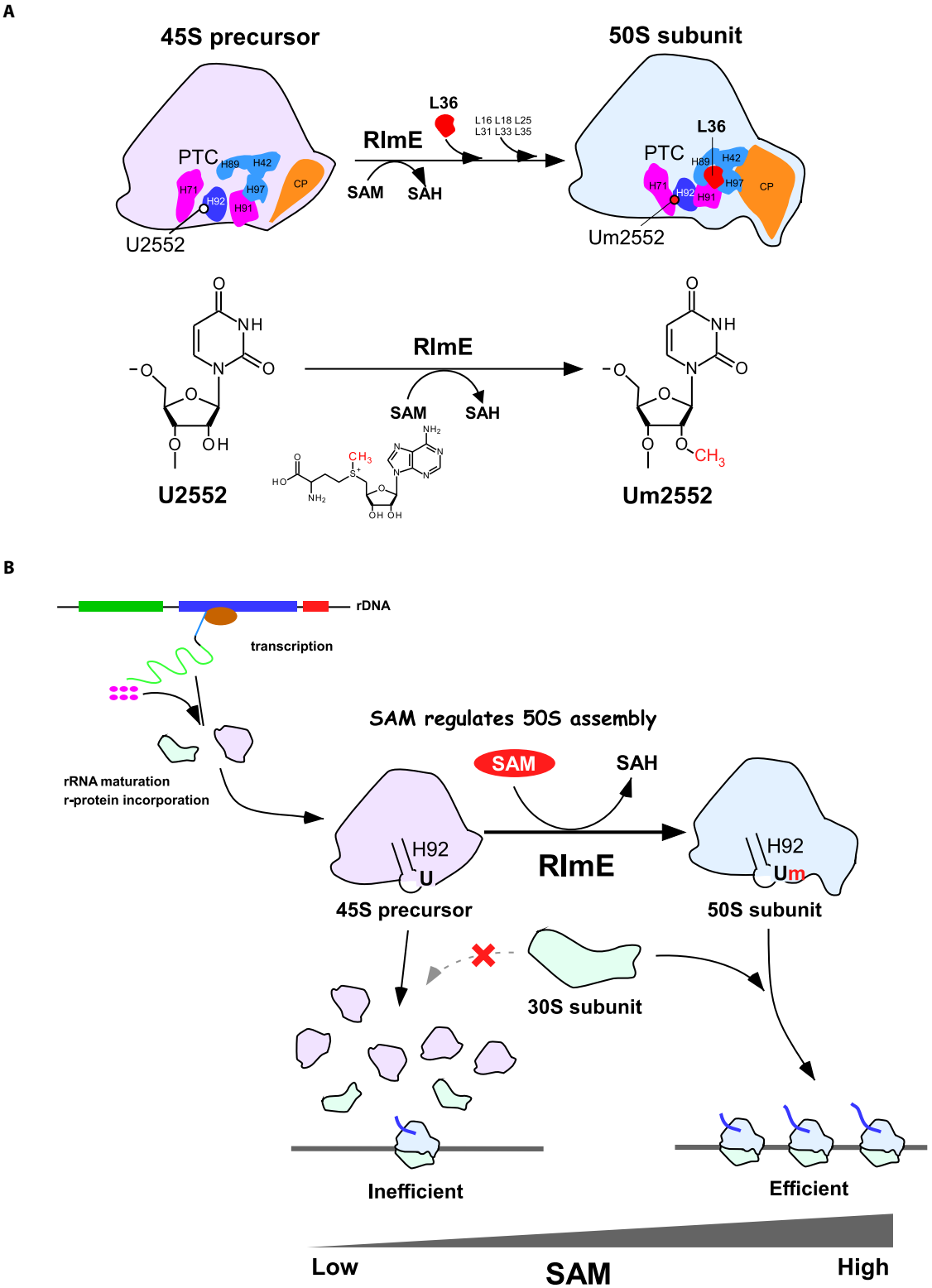

Figure 5. The regulatory role of SAM in 50S assembly. (**A**) Mechanistic model for late assembly of 50S subunits triggered by Um2552 formation. The 45S precursor is a flexible molecule that lacks Um2552 and several r-proteins including L36. RlmE-mediated Um2552 formation promotes the interaction of helices H92 and H71, and incorporation of L36 and other r-proteins. This process triggers 50S maturation in the peptidyl transferase center (PTC) and central protuberance (CP). The chemical scheme of Um2552 formation is shown in the lower figure. SAH, S-adenosyl-L-homocysteine. (**B**) Regulatory mechanism of 50S assembly mediated by Um2552 modification via sensing of the intracellular SAM concentration. When SAM is abundant, RlmE introduces Um2552 into the 45S precursor, which promotes 50S assembly and thereby maintains efficient translation. When SAM is less abundant, Um2552 remains hypomodified and the 45S precursor accumulates, leading to less efficient translation. As the 45S precursor is stably present in cells, 50S subunits can be generated when SAM levels in the cell recover.

plained by 45S accumulation due to Um2552 hypomethylation in the Δ*mtn* strain.

Regarding tRNA modifications, several methyl modifications including m^5U, mnm^5U, ms^2i^6A, Gm and m^7G were down-regulated in the Δ*mtn* strain, indicating that tRNA methyltransferases responsible for these modifications are sensitive to cellular SAM concentration. The modifications m^5U, Gm and m^7G are present at positions 54, 18 and 46, respectively, corresponding to the tRNA core structure. Although gene deletion strains of these methyltransferase exhibited mild phenotypes (55–57), hypomethylation of these sites might influence the stability of tRNA tertiary structure. MiaB is a radical SAM enzyme responsible for methylthiolation of ms^2i^6A at position 37, 3′ adjacent to the tRNA anticodon (58). Because the radical SAM domain utilizes SAM to generate 5′-deoxyadenosyl radical species required for the reaction (59), SAM depletion might affect the radical formation or the methylthiolation as a substrate. The methylthio group of ms^2i^6A37 stacks on the codon–anticodon helix in the decoding center of the ribosome (60), facilitating reading frame maintenance during decoding (61). A decrease in methylthio modification upon SAM depletion might therefore affect the decoding accuracy of tRNAs bearing ms^2i^6A37. In addition to altered methyl modifications, we observed low level of Q and oQ in the Δ*mtn* strain, and accumulation of their precursor preQ1, because SAM is used as a ribosyl donor for Q catalyzed by QueA (62). This observation is consistent with the fact that ribosylation of Q is sensitive to the intracellular SAM concentration (63). Supporting to this finding, the Km value of SAM in this reaction is 98 μM (64), indicating that QueA-mediated oQ formation is regulated by intracellular SAM concentration.

The Um2552 frequency was decreased upon SAM depletion in the Δ*mtn* strain. However, the steady-state level of *rlmE* mRNA was not altered, suggesting that RlmE is a methyltransferase sensitive to cellular SAM concentration. In a previous kinetic study of Um2552 formation using the 50S subunit as a substrate (65), the Km value of SAM was 3.7 μM. Given that the SAM concentration ranges from ∼100 μM in the Δ*mtn* strain to ∼250 μM in WT strain (40), the SAM-sensitive methylation of Um2552 cannot be explained by this *in vitro* kinetic study. This could reflect differences in the reaction conditions *in vitro* and *in vivo*. In addition, the fully assembled 50S subunit was used for kinetic measurement of RlmE *in vitro* (65), even though the 45S precursor is the probable substrate of RlmE *in vivo* (30). To examine this issue, we carried out an *in vitro* methylation assay to compare Um2552 formation of 45S precursor and 50S subunit as substrates. We measured Um2552 frequency by rRNA fragment analysis using RNA-MS. As shown in Supplementary Figure S12, Um2552 efficiently occurred in 50S subunit under low concentration of SAM, whereas Um2552 was not efficiently introduced in 45S precursor under low SAM concentration, and increased with higher SAM concentration. This additional data clearly shows high SAM dependency for Um2552 formation in 45S precursor, and supports our speculation that Um2552 formation is metabolically regulated by cellular SAM concentration.

RlmE is widely conserved in all three domains of life, as well as organelles. In *Saccharomyces cerevisiae*, Spb1p and Mrm2p are homologs of RlmE, and are responsible for rRNA methylation at the corresponding site of cytoplasmic and mitochondrial ribosomes, respectively. Spb1p is an essential protein (66) and the mutation of its SAM-binding site results in a severe cold-sensitive phenotype (67). Deletion of Mrm2p causes thermosensitive respiration and leads to rapid loss of mitochondrial DNA (68). Similar to *E. coli* RlmE, these homologs function during the late stages of ribosome assembly (67,68). In human, FTSJ3 and FTSJ2 are homologs of Spb1p and Mrm2p, respectively (69,70). A loss-of-function mutation in FTSJ2 (MRM2) was detected in a patient displaying MELAS-like mitochondrial dysfunction (71), indicating importance of the rRNA methylation in mitochondrial activity. Given that SAM is an essential metabolite in eukaryotes, and depletion of SAM affects various cellular activities (11,72), SAM-sensitive regulation of ribosome assembly mediated by RlmE homologs might be conserved in eukaryotics. Various phenotypes observed in eukaryotic cell under SAM depleted conditions could therefore be explained by defective ribosome assembly.

Based on our results, we propose that 50S assembly is regulated by Um2552 modification via sensing of the cellular SAM concentration. The 45S precursor is structurally flexible molecule and lacks Um2552 modification, as well as several r-proteins including L36. RlmE-mediated Um2552 formation promotes interdomain interactions via association between helices 92 and 71, and incorporation of L36 and other r-proteins, triggering the final steps of 50S subunit assembly (Figure 5A). When the SAM concentration is high in cells, RlmE facilitates Um2552 modification of the 45S precursor and promotes 50S assembly, generating ribosomes required for efficient translation (Figure 5B). When SAM levels are insufficient, the Um2552 frequency drops and the 45S precursor accumulates, leading to less efficient translation due to lower quantities of the 50S subunit (Figure 5B). Since the 45S precursor is stably accumulated in cells, the 50S subunit can be generated rapidly from the 45S precursor once the intracellular SAM concentration increases. This represents a rapid mechanism for regulating protein synthesis via sensing of the intracellular SAM concentration. Considering that SAM is a central metabolite required for various cellular processes, SAM-sensitive regulation of ribosome biogenesis would be a prerequisite strategy to coordinate cellular activity with translational efficiency.

SUPPLEMENTARY DATA

Supplementary Data are available at NAR Online.

ACKNOWLEDGEMENTS

We thank members of the Suzuki laboratory, especially A. Nagao, S. Kimura, Y. Sakaguchi and K. Miyauchi, for technical assistance and many helpful suggestions.

FUNDING

Grants-in-Aid for Scientific Research on Priority Areas from the Ministry of Education, Culture, Sports, Science

and Technology of Japan [26113003, 26220205, 18H05272 to T.S.]. Funding for open access charge: JSPS; Grants-in-Aid for Scientific Research on Priority Areas from the Ministry of Education, Culture, Sports, Science and Technology of Japan [18H05272 to T.S.].
Conflict of interest statement. None declared.

REFERENCES

1. Fontecave,M., Atta,M. and Mulliez,E. (2004) S-adenosylmethionine: nothing goes to waste. *Trends Biochem. Sci.*, **29**, 243–249.
2. Nishimura,S., Taya,Y., Kuchino,Y. and Oashi,Z. (1974) Enzymatic synthesis of 3-(3-amino-3-carboxypropyl)uridine in Escherichia coli phenylalanine transfer RNA: transfer of the 3-amino-acid-3-carboxypropyl group from S-adenosylmethionine. *Biochem. Biophys. Res. Commun.*, **57**, 702–708.
3. Iwata-Reuyl,D. (2003) Biosynthesis of the 7-deazaguanosine hypermodified nucleosides of transfer RNA. *Bioorg. Chem.*, **31**, 24–43.
4. Casero,R.A. Jr., Murray Stewart,T. and Pegg,A.E. (2018) Polyamine metabolism and cancer: treatments, challenges and opportunities. *Nat. Rev. Cancer*, **18**, 681–695.
5. Bauerle,M.R., Schwalm,E.L. and Booker,S.J. (2015) Mechanistic diversity of radical S-adenosylmethionine (SAM)-dependent methylation. *J. Biol. Chem.*, **290**, 3995–4002.
6. Zhang,Y.M. and Rock,C.O. (2008) Membrane lipid homeostasis in bacteria. *Nat. Rev. Microbiol.*, **6**, 222–233.
7. Broderick,J.B., Duffus,B.R., Duschene,K.S. and Shepard,E.M. (2014) Radical S-adenosylmethionine enzymes. *Chem. Rev.*, **114**, 4229–4317.
8. Janke,R., Dodson,A.E. and Rine,J. (2015) Metabolism and epigenetics. *Annu. Rev. Cell Dev. Biol.*, **31**, 473–496.
9. Li,X., Egervari,G., Wang,Y., Berger,S.L. and Lu,Z. (2018) Regulation of chromatin and gene expression by metabolic enzymes and metabolites. *Nat. Rev. Mol. cell biol.*, **19**, 563–578.
10. Hwang,J.Y., Aromolaran,K.A. and Zukin,R.S. (2017) The emerging field of epigenetics in neurodegeneration and neuroprotection. *Nat. Rev. Neurosci.*, **18**, 347–361.
11. Shiraki,N., Shiraki,Y., Tsuyama,T., Obata,F., Miura,M., Nagae,G., Aburatani,H., Kume,K., Endo,F. and Kume,S. (2014) Methionine metabolism regulates maintenance and differentiation of human pluripotent stem cells. *Cell Metab.*, **19**, 780–794.
12. Bottiglieri,T., Godfrey,P., Flynn,T., Carney,M.W., Toone,B.K. and Reynolds,E.H. (1990) Cerebrospinal fluid S-adenosylmethionine in depression and dementia: effects of treatment with parenteral and oral S-adenosylmethionine. *J. Neurol. Neurosurg. Psychiatry*, **53**, 1096–1098.
13. Jaenisch,R. and Bird,A. (2003) Epigenetic regulation of gene expression: how the genome integrates intrinsic and environmental signals. *Nat. Genet.*, **33**, 245–254.
14. Zhao,B.S., Roundtree,I.A. and He,C. (2017) Post-transcriptional gene regulation by mRNA modifications. *Nat. Rev. Mol. Cell Biol.*, **18**, 31–42.
15. Harcourt,E.M., Kietrys,A.M. and Kool,E.T. (2017) Chemical and structural effects of base modifications in messenger RNA. *Nature*, **541**, 339–346.
16. Roundtree,I.A., Evans,M.E., Pan,T. and He,C. (2017) Dynamic RNA modifications in gene expression regulation. *Cell*, **169**, 1187–1200.
17. Frye,M., Jaffrey,S.R., Pan,T., Rechavi,G. and Suzuki,T. (2016) RNA modifications: what have we learned and where are we headed? *Nat. Rev. Genet.*, **17**, 365–372.
18. Mizushima,S. and Nomura,M. (1970) Assembly mapping of 30S ribosomal proteins from E. coli. *Nature*, **226**, 1214–1218.
19. Herold,M. and Nierhaus,K.H. (1987) Incorporation of six additional proteins to complete the assembly map of the 50 S subunit from Escherichia coli ribosomes. *J. Biol. Chem.*, **262**, 8826–8833.
20. Nierhaus,K.H. (1991) The assembly of prokaryotic ribosomes. *Biochimie.*, **73**, 739–755.
21. Shajani,Z., Sykes,M.T. and Williamson,J.R. (2011) Assembly of bacterial ribosomes. *Annu. Rev. Biochem.*, **80**, 501–526.
22. Iost,I., Bizebard,T. and Dreyfus,M. (2013) Functions of DEAD-box proteins in bacteria: current knowledge and pending questions. *Biochim. Biophys. Acta*, **1829**, 866–877.
23. Britton,R.A. (2009) Role of GTPases in bacterial ribosome assembly. *Annu. Rev. Microbiol.*, **63**, 155–176.
24. Bremer,H. and Dennis,P.P. (2008) Modulation of chemical composition and other parameters of the cell at different exponential growth rates. *EcoSal Plus*, **3**, doi:10.1128/ecosal.5.2.3.
25. Gaca,A.O., Colomer-Winter,C. and Lemos,J.A. (2015) Many means to a common end: the intricacies of (p)ppGpp metabolism and its control of bacterial homeostasis. *J. Bacteriol.*, **197**, 1146–1156.
26. Hauryliuk,V., Atkinson,G.C., Murakami,K.S., Tenson,T. and Gerdes,K. (2015) Recent functional insights into the role of (p)ppGpp in bacterial physiology. *Nat. Rev. Microbiol.*, **13**, 298–309.
27. Strunk,B.S. and Karbstein,K. (2009) Powering through ribosome assembly. *RNA*, **15**, 2083–2104.
28. Caldas,T., Binet,E., Bouloc,P., Costa,A., Desgres,J. and Richarme,G. (2000) The FtsJ/RrmJ heat shock protein of Escherichia coli is a 23 S ribosomal RNA methyltransferase. *J. Biol. Chem.*, **275**, 16414–16419.
29. Bügl,H., Fauman,E.B., Staker,B.L., Zheng,F., Kushner,S.R., Saper,M.A., Bardwell,J.C. and Jakob,U. (2000) RNA methylation under heat shock control. *Mol. Cell*, **6**, 349–360.
30. Arai,T., Ishiguro,K., Kimura,S., Sakaguchi,Y. and Suzuki,T. (2015) Single methylation of 23S rRNA triggers late steps of 50S ribosomal subunit assembly. *Proc. Natl. Acad. Sci. U.S.A.*, **112**, E4707–E4716.
31. Baba,T., Ara,T., Hasegawa,M., Takai,Y., Okumura,Y., Baba,M., Datsenko,K.A., Tomita,M., Wanner,B.L. and Mori,H. (2006) Construction of Escherichia coli K-12 in-frame, single-gene knockout mutants: the Keio collection. *Mol. Syst. Biol.*, **2**, 2006 0008.
32. Datsenko,K.A. and Wanner,B.L. (2000) One-step inactivation of chromosomal genes in Escherichia coli K-12 using PCR products. *Proc. Natl. Acad. Sci. U.S.A.*, **97**, 6640–6645.
33. Barritault,D., Expert-Bezancon,A., Guerin,M.F. and Hayes,D. (1976) The use of acetone precipitation in the isolation of ribosomal proteins. *Eur. J. Biochem.*, **63**, 131–135.
34. Schagger,H. (2006) Tricine-SDS-PAGE. *Nat. Protoc.*, **1**, 16–22.
35. Suzuki,T., Ikeuchi,Y., Noma,A., Suzuki,T. and Sakaguchi,Y. (2007) Mass spectrometric identification and characterization of RNA-modifying enzymes. *Methods Enzymol.*, **425**, 211–229.
36. Sakaguchi,Y., Miyauchi,K., Kang,B.I. and Suzuki,T. (2015) Nucleoside analysis by hydrophilic interaction liquid chromatography coupled with mass spectrometry. *Methods Enzymol.*, **560**, 19–28.
37. Kimura,S., Sakai,Y., Ishiguro,K. and Suzuki,T. (2017) Biogenesis and iron-dependency of ribosomal RNA hydroxylation. *Nucleic Acids Res.*, **45**, 12974–12986.
38. Miyauchi,K., Ohara,T. and Suzuki,T. (2007) Automated parallel isolation of multiple species of non-coding RNAs by the reciprocal circulating chromatography method. *Nucleic Acids Res.*, **35**, e24.
39. Zhou,K., Zhou,L., Lim,Q., Zou,R., Stephanopoulos,G. and Too,H.P. (2011) Novel reference genes for quantifying transcriptional responses of Escherichia coli to protein overexpression by quantitative PCR. *BMC Mol. Biol.*, **12**, 18.
40. Halliday,N.M., Hardie,K.R., Williams,P., Winzer,K. and Barrett,D.A. (2010) Quantitative liquid chromatography-tandem mass spectrometry profiling of activated methyl cycle metabolites involved in LuxS-dependent quorum sensing in Escherichia coli. *Anal. Biochem.*, **403**, 20–29.
41. Ero,R., Peil,L., Liiv,A. and Remme,J. (2008) Identification of pseudouridine methyltransferase in Escherichia coli. *RNA*, **14**, 2223–2233.
42. Popova,A.M. and Williamson,J.R. (2014) Quantitative analysis of rRNA modifications using stable isotope labeling and mass spectrometry. *J. Am. Chem. Soc.*, **136**, 2058–2069.
43. El Yacoubi,B., Bailly,M. and de Crécy-Lagard,V. (2012) Biosynthesis and function of posttranscriptional modifications of transfer RNAs. *Annu. Rev. Genet.*, **46**, 69–95.
44. Miyauchi,K., Kimura,S. and Suzuki,T. (2013) A cyclic form of N6-threonylcarbamoyladenosine as a widely distributed tRNA hypermodification. *Nat. Chem. Biol.*, **9**, 105–111.
45. Dumelin,C.E., Chen,Y., Leconte,A.M., Chen,Y.G. and Liu,D.R. (2012) Discovery and biological characterization of geranylated RNA in bacteria. *Nat. Chem. Biol.*, **8**, 913–919.
46. Esberg,B., Leung,H.C., Tsui,H.C., Björk,G.R. and Winkler,M.E. (1999) Identification of the miaB gene, involved in methylthiolation of isopentenylated A37 derivatives in the tRNA of Salmonella typhimurium and Escherichia coli. *J. Bacteriol.*, **181**, 7256–7265.

47. Slany,R.K., Bösl,M. and Kersten,H. (1994) Transfer and isomerization of the ribose moiety of AdoMet during the biosynthesis of queuosine tRNAs, a new unique reaction catalyzed by the QueA protein from Escherichia coli. *Biochimie.*, **76**, 389–393.
48. Wion,D. and Casadesus,J. (2006) N6-methyl-adenine: an epigenetic signal for DNA-protein interactions. *Nat. Rev. Microbiol.*, **4**, 183–192.
49. Luo,G.Z., Blanco,M.A., Greer,E.L., He,C. and Shi,Y. (2015) DNA N(6)-methyladenine: a new epigenetic mark in eukaryotes? *Nat. Rev. Mol. Cell Biol.*, **16**, 705–710.
50. Sergiev,P.V., Aleksashin,N.A., Chugunova,A.A., Polikanov,Y.S. and Dontsova,O.A. (2018) Structural and evolutionary insights into ribosomal RNA methylation. *Nat. Chem. Biol.*, **14**, 226–235.
51. Polevoda,B. and Sherman,F. (2007) Methylation of proteins involved in translation. *Mol. Microbiol.*, **65**, 590–606.
52. Andersen,N.M. and Douthwaite,S. (2006) YebU is a m5C methyltransferase specific for 16 S rRNA nucleotide 1407. *J. Mol. Biol.*, **359**, 777–786.
53. Basturea,G.N. and Deutscher,M.P. (2007) Substrate specificity and properties of the Escherichia coli 16S rRNA methyltransferase, RsmE. *RNA*, **13**, 1969–1976.
54. Madsen,C.T., Mengel-Jorgensen,J., Kirpekar,F. and Douthwaite,S. (2003) Identifying the methyltransferases for m(5)U747 and m(5)U1939 in 23S rRNA using MALDI mass spectrometry. *Nucleic Acids Res.*, **31**, 4738–4746.
55. Urbonavicius,J., Durand,J.M. and Bjork,G.R. (2002) Three modifications in the D and T arms of tRNA influence translation in Escherichia coli and expression of virulence genes in Shigella flexneri. *J. Bacteriol.*, **184**, 5348–5357.
56. Bjork,G.R. and Neidhardt,F.C. (1975) Physiological and biochemical studies on the function of 5-methyluridine in the transfer ribonucleic acid of Escherichia coli. *J. Bacteriol.*, **124**, 99–111.
57. De Bie,L.G., Roovers,M., Oudjama,Y., Wattiez,R., Tricot,C., Stalon,V., Droogmans,L. and Bujnicki,J.M. (2003) The yggH gene of Escherichia coli encodes a tRNA (m7G46) methyltransferase. *J. Bacteriol.*, **185**, 3238–3243.
58. Pierrel,F., Bjork,G.R., Fontecave,M. and Atta,M. (2002) Enzymatic modification of tRNAs: MiaB is an iron-sulfur protein. *J. Biol. Chem.*, **277**, 13367–13370.
59. Kimura,S. and Suzuki,T. (2015) Iron-sulfur proteins responsible for RNA modifications. *Biochim. Biophys. Acta*, **1853**, 1272–1283.
60. Jenner,L.B., Demeshkina,N., Yusupova,G. and Yusupov,M. (2010) Structural aspects of messenger RNA reading frame maintenance by the ribosome. *Nat. Struct. Mol. Biol.*, **17**, 555–560.
61. Urbonavicius,J., Qian,Q., Durand,J.M., Hagervall,T.G. and Bjork,G.R. (2001) Improvement of reading frame maintenance is a common function for several tRNA modifications. *EMBO J.*, **20**, 4863–4873.
62. Slany,R.K., Bosl,M., Crain,P.F. and Kersten,H. (1993) A new function of S-adenosylmethionine: the ribosyl moiety of AdoMet is the precursor of the cyclopentenediol moiety of the tRNA wobble base queuine. *Biochemistry*, **32**, 7811–7817.
63. Okada,N., Yasuda,T. and Nishimura,S. (1977) Detection of nucleoside Q precursor in methyl-deficient E.coli tRNA. *Nucleic Acids Res.*, **4**, 4063–4075.
64. Van Lanen,S.G. and Iwata-Reuyl,D. (2003) Kinetic mechanism of the tRNA-modifying enzyme S-adenosylmethionine:tRNA ribosyltransferase-isomerase (QueA). *Biochemistry*, **42**, 5312–5320.
65. Hager,J., Staker,B.L., Bugl,H. and Jakob,U. (2002) Active site in RrmJ, a heat shock-induced methyltransferase. *J. Biol. Chem.*, **277**, 41978–41986.
66. Kressler,D., Rojo,M., Linder,P. and Cruz,J. (1999) Spb1p is a putative methyltransferase required for 60S ribosomal subunit biogenesis in Saccharomyces cerevisiae. *Nucleic Acids Res.*, **27**, 4598–4608.
67. Lapeyre,B. and Purushothaman,S.K. (2004) Spb1p-directed formation of Gm2922 in the ribosome catalytic center occurs at a late processing stage. *Mol. Cell*, **16**, 663–669.
68. Pintard,L., Bujnicki,J.M., Lapeyre,B. and Bonnerot,C. (2002) MRM2 encodes a novel yeast mitochondrial 21S rRNA methyltransferase. *EMBO J.*, **21**, 1139–1147.
69. Rorbach,J., Boesch,P., Gammage,P.A., Nicholls,T.J., Pearce,S.F., Patel,D., Hauser,A., Perocchi,F. and Minczuk,M. (2014) MRM2 and MRM3 are involved in biogenesis of the large subunit of the mitochondrial ribosome. *Mol. Biol. Cell*, **25**, 2542–2555.
70. Morello,L.G., Coltri,P.P., Quaresma,A.J., Simabuco,F.M., Silva,T.C., Singh,G., Nickerson,J.A., Oliveira,C.C., Moore,M.J. and Zanchin,N.I. (2011) The human nucleolar protein FTSJ3 associates with NIP7 and functions in pre-rRNA processing. *PLoS One*, **6**, e29174.
71. Garone,C., D'Souza,A.R., Dallabona,C., Lodi,T., Rebelo-Guiomar,P., Rorbach,J., Donati,M.A., Procopio,E., Montomoli,M., Guerrini,R. *et al.* (2017) Defective mitochondrial rRNA methyltransferase MRM2 causes MELAS-like clinical syndrome. *Hum. Mol. Genet.*, **26**, 4257–4266.
72. Kishita,Y., Pajak,A., Bolar,N.A., Marobbio,C.M., Maffezzini,C., Miniero,D.V., Monne,M., Kohda,M., Stranneheim,H., Murayama,K. *et al.* (2015) Intra-mitochondrial methylation deficiency due to mutations in SLC25A26. *Am. J. Hum. Genet.*, **97**, 761–768.